A non-enzymatic amperometric hydrogen peroxide sensor based on iron nanoparticles decorated on reduced graphene oxide nanocomposite

Baishnisha Amanulla[a], Selvakumar Palanisamy[b], Shen-Ming Chen[a]*, Vijaylakshmi Velusamy[c]**, Te-Wei Chiu[d]***, Tse-Wei Chen[a], Sayee Kannan Ramaraj[a, c]*****

[a]PG & Research department of Chemistry, Thiagarajar College, Madurai-09, Tamilnadu, India.

[b]Electroanalysis and Bioelectrochemistry Lab, Department of Chemical Engineering and Biotechnology, National Taipei University of Technology, No. 1, Section 3, Chung-Hsiao East Road, Taipei 106, Taiwan, ROC.

[c]Division of Electrical and Electronic Engineering, School of Engineering, Manchester Metropolitan University, Manchester – M1 5GD, United Kingdom.

[d]Department of Materials and Mineral Resources Engineering, National Taipei University of Technology, 1, Sec. 3, Zhongxiao E. Rd., Taipei 106, Taiwan.

Corresponding Authors:

*S.M. Chen, E-mail: smchen78@ms15.hinet.net

**V. Velusamy, E-mail: V.Velusamy@mmu.ac.uk

*** T.W. Chiu, E-mail: tewei@ntut.edu.tw

****R. Sayee Kannan, E-mail: sayeekannanramaraj@gmail.com

Abstract

A simple and facile green process was used for the synthesis of iron nanoparticles (FeNPs) decorated reduced graphene oxide (rGO) nanocomposite by using *Ipomoea pes-tigridis* leaf extract as a reducing and stabilizing agent. The as-prepared rGO/FeNPs nanocomposite was characterized by transmission electron microscopy, X-ray spectroscopy and Fourier transform infrared spectroscopy. The nanocomposite was further modified on the glassy carbon electrode and used for non-enzymatic sensing of hydrogen peroxide (H_2O_2). Cyclic voltammetry results reveal that rGO/FeNPs nanocomposite has excellent electro-reduction behavior to H_2O_2 when compared to the response of FeNPs and rGO modified electrodes. Furthermore, the nanocomposite modified electrode shows 9 and 6 folds enhanced reduction current response to H_2O_2 than that of rGO and FeNPs modified electrodes. Amperometric method was further used to quantify the H_2O_2 using rGO/FeNPs nanocomposite, and the response of was linear over the concentration ranging from 0.1 µM to 2.15 mM. The detection limit and sensitivity of the sensor were estimated as 0.056 µM and 0.2085 $\mu A \mu M^{-1} cm^{-2}$, respectively. The fabricated sensor also utilized for detection of H_2O_2 in the presence of potentially active interfering species, and found high selectivity towards H_2O_2.

Keywords: Reduced graphene oxide; Iron nanoparticles; *Ipomoea pes-tigridis* leaf extract; hydrogen peroxide; non-enzymatic sensor.

1. Introduction

Recent years, the magnetic nanoparticles have received great interest in the scientific community due to their unique physical and chemical properties associated with remarkable magnetic behavior [**1**]. In particular, iron nanoparticles (FeNPs) has been widely used for different potential applications such as magnetic storage media [**2**], ferrofluids [**3**], biosensors [**4**], catalysts [**5**], and environment remediation [**6**]. In addition, FeNPs has also been used as a promising electrocatalyst in electrochemical sensors [**7, 8**]. So far, different synthetic protocols have been used for synthesis of FeNPs, such as vacuum sputtering [9], decomposition in organic solvents [**10**] and chemical reduction [**11**]. Furthermore, the stabilizers such as chitosan [**12**], activated carbon [**13**] and carboxymethyl cellulose [**14**] have also been used to synthesize the stable and small sized FeNPs. Usually, the FeNPs are produced by chemical reduction methods owing to its simplicity and feasibility [15]. However, the chemical reduction methods are toxic, corrosive and non-eco-friendly. To conquer this problem, nowadays a simple, cost effective and environmentally friendly new methods being more preferred. On the other hand, reduced graphene oxide (rGO) has emerged in various fields due to its high conductivity, large surface area and chemical inertness [**16, 17**]. Despite of the unique properties of rGO, it has continually received much attention in electrochemical sensors and biosensors [**18–20**]. Different methods have been adopted for synthesis of graphene oxide to rGO, such as thermal reduction, chemical reduction, solvothermal reduction, photocatalytic reduction, bio-reduction and electrochemical reduction [**21**]. Compared to other methods, bio-reduction of rGO is more attractive due to its low cost and short time [**22**]. Recently, rGO and rGO composites have been prepared by bio-reduction methods using plant extracts of spinach, tea and vegetables [**23–25**]. The motivation of the present work is to synthesize FeNPs decorated rGO (rGO/FeNPs) nanocomposite using the *Ipomoea pes-tigridis* leaf extract as a reducing and stabilizing agent.

Hydrogen peroxide (H_2O_2) is widely applied in range of applications such as pulp and paper-bleaching and production of various organic peroxides in industries [**26, 27**]. It is also used as essential mediator in food, pharmaceutical, clinical, industrial and environmental analyses [**27**]. Different analytical methods have been developed for quantification of H_2O_2 including such as spectrophotometry, titrimetry, chemiluminescence, fluorescence, colorimetry, and electrochemical methods [**27–32**]. Compared with other methods, electrochemical methods have been widely used for quantification of H_2O_2 due to its easy operation, low cost, high sensitivity and selectivity [**33**]. Heme redox active proteins have also widely used for construction of H_2O_2 biosensors due to their high selectivity towards H_2O_2 [**34–37**], though the stability and complicated immobilization procedures of these biosensors lead to limited interest in the scientific community [**33**]. As alternative, non-enzymatic H_2O_2 sensors have been developed with the use of metal and metal alloy nanoparticles, metal oxides, conducting polymers, carbon micro and nanomaterials including FeNPs and rGO [**38, 39**].

In this present work, a sensitive and selective non-enzymatic H_2O_2 sensors was developed using rGO/FeNPs nanocomposite modified electrode for the first time. *Ipomoea pes-tigridis* leaf extract is used as a reducing and capping agent for synthesis of rGO/FeNPs nanocomposite. The effects rGO/FeNPs nanocomposite loading, scan rate and pH towards H_2O_2 have been studied and discussed. Other crucial parameters, such as reproducibility and repeatability have also been critically studied and discussed. The practical ability of the sensor was examined in commercial contact lens solution, human serum and urine samples and results also critically discussed in the manuscript.

2. Experimental

2.1. Materials and method

Natural graphite powder (<20 μm, synthetic), sodium nitrate, potassium permanganate and ferric chloride were purchased from Sigma-Aldrich, India. Hydrogen peroxide (30%) was obtained from Sigma-Aldrich, Taiwan, and used as received. *Ipomoea pes-tigridis* leaf (IPT) was collected from the local area in Madurai, Tamil Nadu. All aqueous solutions used in this work were prepared by deionized water. pH 7.0 (PBS) was used as the supporting electrolyte for all experiments and prepared by using 0.05 mol L^{-1} Na_2HPO_4 and NaH_2PO_4 solutions in doubly distilled water. The pH was adjusted using diluted NaOH and H_2SO_4.

The morphological studies of the as-synthesized materials were characterized by FEI Tecnai G2 20 S-TWIN transmission electron microscopy with an accelerating voltage of 200 kV. The crystallographic nature of the materials was studied by a powder X-ray diffraction (XRD) from Panalytical X' per PRO X-ray diffractometer equipped with Cu Kα radiation (λ = 0.15406 nm). Fourier transform infrared spectroscopy (FTIR) was performed by a Shimadzu model FT-IR spectrometer. Electrochemical measurements were carried out by CHI 1205A electrochemical analyzer from CH Instruments. Typical three electrode configuration was used for electrochemical studies where glassy carbon electrode (GCE) with a geometric surface area of 0.079 cm^2 as a working electrode and a saturated Ag/AgCl and Pt wire used as a reference and counter electrodes respectively. Rotating ring disc electrode (RDE) with a geometric area about 0.24 cm^2 was used for amperometric measurements and was performed by PRDE-3A (AS distributed by BAS Inc. Japan). All electrochemical measurements were carried out at a room temperature under N_2 atmosphere.

2.2. Synthesis of rGO/FeNPs composite

To prepare *Ipomoea pes-tigridis* leaf extract, fresh *Ipomoea pes-tigridis* leaf was washed and cleaned by double distilled water and cut into small pieces. The aqueous extract of *Ipomoea pes-*

tigridis leaf extract (IPTLE) was prepared by the addition of 1 g of leaf with 100 mL of distilled water at 90 ^{0}C for 15 min, which is similar to our reported procedure for leaf extract preparation. The obtained leaf extract was filtered and preserved in a refrigerator (10 $^{\circ}$C). Graphene oxide was prepared from the natural graphite by previously reported method elsewhere [**33**]. To prepare rGO/FeNPs nanocomposite, 50 µL of as-prepared GO suspension (1 mg mL^{-1}) was added into the 50 mL of 1 mM $FeCl_3$ solution. The mixture was stirred for 10 min to complete the ion exchange reaction. Then, 100 mL of freshly prepared IPTLE was added dropwise into solution with constant stirring up to 10 min. Finally, the yellow solution turns into the black dispersion, which signifies the successful reduction of Fe^{3+} to Fe^{0} and GO to rGO respectively. The obtained rGO/FeNPs composite was separated by centrifugation and washed with doubly distilled water and dried in a vacuum oven at 50 $^{\circ}$C for 24 h. The rGO and FeNPs were prepared by similar aforementioned method without $FeCl_3$ and GO. The rGO/FeNPs nanocomposite dispersion (1 mg mL^{-1}) was prepared by using doubly distilled water with aid of sonication about 15 min. The schematic representation for the preparation of rGO/FeNPs nanocomposite using IPTLE is shown in **Scheme 1**.

To prepare rGO/FeNPs nanocomposite modified electrode, about 6 mL of rGO/FeNPs nanocomposite dispersion (see **Fig. 4A inset** for optimization studies) was coated on the pre-cleaned GCE and dried at room temperature. The other modified electrodes such as FeNPs and RGO were prepared by drop coating of 8 µL FeNPs and RGO on unmodified GCE and dried in the room temperature. All electrodes were stored under dry condition in room temperature when not in use.

3. Results and Discussion

3.1. Characterizations

The surface morphology and structure of as-prepared nanomaterials were characterized by TEM and representative TEM images are shown in **Fig. 1**. The TEM image of FeNPs (**Fig. 1A**) show that the uniform and spherical FeNPs with an average diameter about 26 ± 2 nm. On the other hand, the TEM image of rGO (**Fig. 1B**) shows a thin sheet like morphology with an association of few layers. The TEM image of rGO/FeNPs (**Fig. 1C**) reveal that FeNPs are in irregular shape and decorated uniformly on the surface of rGO nanosheets. In addition, the observed diameter of FeNPs (28 ± 4) in the nanocomposite is consistent with the TEM image of FeNPs. The result indicates the formation of rGO/FeNPs nanocomposite. The EDX spectrum was also performed to investigate elemental distribution of the rGO/FeNPs nanocomposite and its corresponding EDX spectrum is shown in **Fig. 1D**. The EDX spectrum were confirmed the presence of C, O, K and Fe, which are due to rGO/FeNPs and leaf extract, since the K is an essential element for plant growth. The result supports the presence of FeNPs on rGO surface.

FTIR spectroscopy was used to analyzed the possible biomolecules responsible for the reduction and stabilization of rGO/FeNPs composite. **Fig. 2A** illustrates the FTIR spectrum of IPTLE and shows the strong adsorption bands at 3450, 1650 and 1042 cm^{-1} corresponds to the –OH stretching vibration of poly phenols, stretching vibrations of C=O from carbonyl and carboxyl groups and stretching vibration of C–O from ester [**40**]. In addition, bands at 2901, 2832 and 1440 cm^{-1} are due to the –NH stretching vibrations of amide, stretching vibrations C=H of aldehydic amine and –CH stretching vibrations of proteins [**40**]. The result confirmed that IPTLE contains high amount of phenol, aromatic amines, proteins, aldehyde, polyol and methylene groups. The FTIR spectra of GO, rGO and rGO/FeNPs is shown in **Fig. 2B**. The FTIR spectrum of GO demonstrate a broad intense band at 3300-3500 cm^{-1} which is due to the stretching vibration of carboxylic acid group and intercalated water molecules [**33**]. The characteristic band of C=O

groups in carbonyl and carbonyl moieties is observed at 1720 cm^{-1} [**33**]. In addition, C-OH band at 1318 cm^{-1}, epoxy or alkoxy C-O stretches at 1060 cm^{-1} were also observed. The result confirms the successful oxidation of graphite into GO. The FTIR spectrum of rGO reveal that most of oxygen containing functional groups in GO were successfully removed after the reaction with IPTLE. The bands related to C=O and –OH (3300-3500 cm^{-1}) were reduced dramatically and only the band at 1620 cm^{-1} remains observed [**33**]. The results confirm the successful reduction of GO to rGO by IPTLE. It is also noted that the observed FTIR spectrum of rGO/FeNPs nanocomposite is similar to the FTIR spectrum of rGO, which indicating the presence of rGO. However, FTIR spectrum of rGO/FeNPs nanocomposite shows a weak band at 600-700 cm^{-1} is possibly due to the inevitable oxidation of FeNPs when exposure to air [**41**].

The formation of FeNPs-rGO composites further confirmed by XRD. The XRD patterns of GO, rGO, FeNPs and FeNPs-rGO composite shown in **Fig 3**. XRD Pattern of GO (curve a) exhibits a strong diffraction peaks at $2\theta = 10.21^{\circ}$, corresponding to the (001) reflection of GO [**42**]. While, the diffraction peak at 10° was disappeared in rGO (curve b), which confirm the efficient reduction of GO. It is interesting to note that rGO exhibits a strong diffraction peak at $2\theta = 24.3^{\circ}$ and 42.5^{o}, which confirm the presence of few layers rGO [**42**]. On the other hand, the XRD pattern of FeNPs (curve c) and rGO/FeNPs (curve d) composite shows main reflection peaks at $2\theta = 44.8$ and 68.0°, which are the characteristic peaks of cubic Fe (JCPDS, file No. 06-0696). The average particle size of FeNPs in rGO/FeNPs was calculated using Scherrer's equation. The average particle size of FeNPs was found as 28.4 nm and was more consistent with the TEM results.

3.2. Electrocatalytic activity of rGO/FeNPs composite towards reduction of H_2O_2

The electrocatalytic activity of different modified electrode towards reduction of H_2O_2 was evaluated using CV. **Fig. 4A** shows CV response of bare (a), FeNPs (b), rGO (c) and rGO/FeNPs

nanocomposite (d) modified electrodes in N_2 saturated PBS containing 1 mM H_2O_2 at a scan rate of 50 mV/s. The potentials were scanned in the range between 0.2 to –0.8 V. The bare electrode did not show any response for the presence of H_2O_2, which indicates that the unmodified electrode is not suitable for detection of H_2O_2. The RGO and FeNPs modified electrodes show a sharp reduction peak at -0.607 and 0.51 V for H_2O_2 at the same potential window. In addition, the observed reduction peak current for H_2O_2 of both electrodes were found similar. On the other hand, rGO/FeNPs nanocomposite modified electrode shows a well-defined reduction peak current at -0.507 V, and the observed reduction current response was about 3 folds higher than those observed in rGO and FeNPs modified electrodes. Furthermore, rGO/FeNPs nanocomposite modified electrode shows 0.1 V lower reduction potential for H_2O_2 when compared to rGO modified electrode. The result validates that rGO/FeNPs nanocomposite modified electrode has high electrocatalytic activity towards the reduction of H_2O_2 than that of other modified electrodes and can be used for quantification of H_2O_2. As shown in **Fig. 4A inset**, the best response of rGO/FeNPs nanocomposite modified electrode for H_2O_2 was observed in 6 µL drop coated composite modified electrode. Hence, it is used as an optimum for further studies.

We have also investigated the electrocatalytic activity of rGO/FeNPs nanocomposite modified electrode in the absence and presence of H_2O_2 and the results are shown in **Fig. 4B**. In the absence of H_2O_2, the composite modified electrode did not show any apparent response in PBS. While, a sharp reduction peak was observed at -0.507 V for the presence of 1 mM H_2O_2 containing PBS. The result reveals the typical electro-reduction ability of rGO/FeNPs nanocomposite modified electrode towards H_2O_2. The FeNPs has played an important role with rGO and result into the enrichment of reduction peak signal of H_2O_2 than that of individual FeNPs and RGO. Usually, the reduction of H_2O_2 involving the generation of hydroxyl radicals and superoxide. The generated

compounds (hydroxyl radicals and superoxide) can react with FeNPs (Fe^{III}/Fe^{II}) and result into the reduction of H_2O_2 to water and oxygen. The enrichment of the reduction peak of H_2O_2 is possibly from the high conductivity of rGO and high catalytic ability of FeNPs.

Fig. 5A shows effect of different scan rate on the CV response of rGO/FeNPs nanocomposite modified electrode for 1 mM H_2O_2 containing PBS. The scan rates were in the range of 20–180 mV/s (a–i). It can be seen that the reduction peak current response of H_2O_2 increases with increasing the scan rates from 20 to 180 mV/s. In addition, the cathodic peak was shifted towards negative direction upon increasing the scan rates. As shown in **Fig. 5A inset**, the cathodic peak current of H_2O_2 had a linear dependence over the square root of scan rates from 20 to 180 mV/s with the correlation coefficient of 0.9961. The result indicates that the reduction of H_2O_2 on rGO/FeNPs nanocomposite modified electrode is a typical diffusion controlled electrochemical process [**43**]. We have also investigated the influence of pH on the electrocatalytic reduction behavior of rGO/FeNPs nanocomposite modified electrode towards H_2O_2. **Fig. 5B** displays the effect of pH vs. reduction peak current of 1 mM H_2O_2 on rGO/FeNPs nanocomposite modified electrode. The experimental conditions are similar to **Fig. 5A**. Fig. 4B clears that a maximum sensitivity for H_2O_2 was observed in pH 7, and the sensitivity was decreases when the pH was above or below 7. The pH sensitivity of the rGO/FeNPs nanocomposite modified electrode H_2O_2 was calculated as 0.1006, 0.2217, 0.3826, 0.4783, 0.3913 and 0.4478 mA/cm for pH 1, 3, 5, 7, 9 and 11, respectively. The electrochemical active surface area (ESCA) of the electrode was 0.23 cm^2, and calculated using Randles–Sevcik equation. The maximum pH sensitivity of the composite electrode towards H_2O_2 was observed at pH 7 than other pH, which is due to the high stability of the composite in natural pH than other pH. In addition, pH 7 as an appropriate pH for the composite

electrode towards practical applications. Therefore, we chosen pH 7 as an optimum for electrocatalytic measurements.

3.3. Amperometric determination of H_2O_2

An amperometric *i-t* method was used for the determination of H_2O_2 using rGO/FeNPs nanocomposite modified RDE. It is well known that amperometric method is an ideal method for non-enzymatic sensors due to its higher sensitivity and fast response. **Fig. 6** shows typical amperometric response of rGO/FeNPs nanocomposite modified RDE for addition of different concentrations of H_2O_2 (0.3 to 77.55 µM) into the constantly stirred PBS at the working potential of -0.5 V. The operational potential was selected from the CV measurements of **Fig. 4A**. It can be seen from **Fig. 6 upper inset**, a well-defined amperometric response was observed for the addition of 0.1 (a), 0.5 (b) and 1 (c) µM H_2O_2 into PBS. It is also note that a sharp response was observe for the addition of 5 (d), 15 (e) and 50 (f) µM H_2O_2. The result indicates the excellent electrocatalytic reduction ability of rGO/FeNPs nanocomposite modified RDE towards H_2O_2. The response of the H_2O_2 was reached within 2 s for the addition of 5 (d), 15 (e) and 50 (f) µM H_2O_2, which indicates the fast diffusion of H_2O_2 on the composite modified electrode. The amperometric response of the modified electrode was linear over the concentration of H_2O_2 ranging from 0.1 µM to 2.15 mM with the correlation coefficients of 0.9911 (**Fig. 6 lower inset**). The sensitivity of the sensor was calculated as 0.2085 µA $\mu M^{-1}cm^{-2}$, which is calculated from the slope of the calibration plot/ ESCA of the rGO/FeNPs nanocomposite modified RDE. The ESCA of the composite modified electrode is determined as 0.47 cm^2, and was calculated using Randles–Sevcik equation. The detection limit (LOD) of the sensor was calculated as 0.056 µM based on (3 ∗ Sd of the blank response)/slope of the calibration plot. On the other hand, the sensitivity and LOD for FeNPs modified electrode were calculated as 0.065 µA $\mu M^{-1}cm^{-2}$ and 1.6 µM (figure not presented here). The sensitivity of

rGO/FeNPs nanocomposite electrode was 3 folds enhanced when the FeNPs combined with rGO, which is due to high surface area and high conductivity of rGO. In addition, the LOD of the composite modified electrode was deduced to sub-micro molar levels (56 nM) when compared to the LOD of FeNPs (1.6 µM). The result clearly indicates that the sensitivity and LOD of the sensor is greatly improved in the rGO/FeNPs nanocomposite, which is resulting from the combined unique properties of rGO and FeNPs. It is also noted that the obtained LOD (0.056 µM) of the sensor is much lower than previously reported non-enzymatic H_2O_2 sensors, as shown in **Table. 1**. Furthermore, the linear response range (0.1 µM to 2.15 mM) and applied potential (–0.5 V) of the sensor are more comparable with the recently reported H_2O_2 sensors [**8, 44–48**]. Hence, rGO/FeNPs nanocomposite modified electrode can be used as a sensitive electrode material for quantification of H_2O_2.

The selectivity of modified electrode is vital for non-enzymatic H_2O_2 sensors; hence, we have evaluated the selectivity of rGO/FeNPs nanocomposite modified electrode for detection of H_2O_2 in the presence of potentially active electroactive compounds such as dopamine (DA), uric acid (UA), ascorbic acid (AA), catechol (CT) and glucose. **Fig. 7** shows amperometric *i-t* response of rGO/FeNPs nanocomposite modified RDE for the addition of 1 µM H_2O_2 (a), and 100 µM addition of DA (b), UA (c), catechol (d), AA (e) and glucose (f) into the constant stirred N_2 saturated PBS at a working potential of -0.5 V. The high negative working potential (-0.5 V) is more beneficial for selective sensing of H_2O_2 [**33**]. It can be seen that most of the interfering species did not show any apparent amperometric signal on the modified electrode. It is also note that AA shows a tiny amperometric response on the composite modified electrode. However, the observed response of the AA is negligible when compared to the amperometric response of H_2O_2. The above result proved the high selectivity of rGO/FeNPs nanocomposite towards the detection of H_2O_2, and it

also reveals that the composite modified electrode can be used for selective sensing of H_2O_2 in complex matrix.

To evaluate the practical ability of the sensor, the rGO/FeNPs nanocomposite modified electrode was used for the detection of H_2O_2 in human serum, urine and commercial contact lens solution samples. Amperometric i-t method was used for the detection of H_2O_2 and the experimental conditions are similar as of in **Fig. 6**. The standard addition method was used for the calculation of recovery of H_2O_2 in human serum, urine and commercial contact lens solution samples [**62**]. First the unknown concentration of commercial contact lens solution (3%) was predetermined and known concentration of solution was further injected into the PBS. The recovery values were summarized in **Table 2**, and the recoveries were 98.5, 97.3, and 101.0 % in commercial contact lens solution, human serum and urine samples. The result substantiates the potential ability of rGO/FeNPs nanocomposite modified electrode towards the detection of H_2O_2 in biological and pharmaceutical samples.

We have also tested the reproducibility and repeatability of the sensor using CV and the experimental conditions are similar to **Fig. 4A**. The relative standard deviation (RSD) of 3.6% was found for detection of 1 mM H_2O_2 using five rGO/FeNPs nanocomposite modified electrode. On the other hand, a single composite modified electrode for detection of 8 set of 1 mM H_2O_2 containing PBS shows the RSD about 2.6%. The result also validates that the as-developed sensor has appropriate reproducibility and repeatability for detection of H_2O_2.

4. Conclusions

In summary, we have developed a sensitive and selective non-enzymatic amperometric H_2O_2 sensor using the composite of rGO/FeNPs for the first time. The physicochemical results confirmed the successful formation of rGO/FeNPs composite. TEM images showed that the FeNPs

were evenly distributed on rGO surface with an average diameter of 28 ± 4 nm. The rGO/FeNPs composite exhibited an excellent electrocatalytic activity towards reduction of H_2O_2 at –0.5 V. In addition, the developed H_2O_2 sensor showed an advanced analytical features such as low LOD (0.056 µM), high sensitivity (0.2086 µA $\mu M^{-1}cm^{-2}$), fast response (2 s) and wide linear response (up to 2.15 mM) for detection of H_2O_2. The excellent practicality of rGO/FeNPs composite in human serum, urine and commercial contact lens solutions substantiates that its potential application towards sensing of H_2O_2 in real samples.

Acknowledgments

This project was supported by the National Science Council and the Ministry of Education of Taiwan (Republic of China). One of the author, Dr. R. Sayee Kannan greatly acknowledge the management of Thiagarajar College, Madurai for giving the permission to visit NTUT, Taiwan as research professor.

References

[1] D. L. Huber, Small 1 (2005) 482–501.

[2] S.H. Sun, C.B. Murray, D. Weller, L. Folks, A. Moser, Science 287 (2000) 1989–1992.

[3] K. Raj, B. Moskowitz, R. Casciari, J. Magn. Mater. 149 (1995) 174–180.

[4] M.M. Miller, G.A. Prinz, S.F. Cheng, S. Bounnak, Appl. Phys. Lett. 81 (2002) 2211–2213.

[5] J.L. Zhang, Y. Wang, H. Ji, Y.G. Wei, N.Z. Wu, B.J. Zuo, Q.L. Wang, J. Catal. 229 (2005) 114–118.

[6] J. Fan, Y.H. Guo, J.J. Wang, M.H. Fan, J. Hazard. Mater. 166 (2009) 904–910.

[7] H. Mei, W. Wu, B. Yu, H. Wu, S. Wang, Q. Xia, Sens. Actuators, B, 223 (2016) 68–75.

[8] O. Akyıldırım, H. Medetalibeyoğlu, S. Manap, M. Beytur, F.S. Tokalı, M.L. Yola, N. Atar, Int. J. Electrochem. Sci., 10 (2015) 7743–7753.

[9] L.T. Kuhn, A. Bojesen, L. Timmermann, M.M. Nielsen, S. Morup, J Phys Condens Matter, 14 (2002) 13551–67.

[10] M.N.A. Karlsson, K. Deppert, B.A. Wacaser, L.S. Karlsson, J.O. Malm, J. Appl. Phys A: Mater Sci Process 80 (2005) 1579–83.

[11] C.B. Wang, W.X. Zhang, Environ Sci Technol. 31 (1997) 2154 –60.

[12] B. Geng, Z.H. Jin, T.L. Li, X.H. Qi, Sci. Total Environ. 07 (2009) 4994–5000.

[13] H.J. Zhu, Y.F. Jia, X. Wu, H. Wang, J. Hazard. Mater. 172 (2009) 1591–1596.

[14] Q. Wang, H.J. Qian, Y.P. Yang, Z. Zhang, C. Naman, X.H. Xu, J. Contam. Hydrol. 114 (2010) 35–42.

[15] T. Shahwan, S.A. Sirriah, M. Nairat, E. Boyacı, A.E. Eroğlu, T.B. Scott, K.R. Hallam, J. Chem Eng. 172 (2011) 258–66.

[16] Y. Wang, Z. Li, J. Wang, J. Li and Y. Lin, Trends Biotechnol., 29 (2011) 205–212.

[17] Y. Zhu, S. Murali, W. Cai, X. Li, J. Suk, J.R. Potts, R.S. Ruof, Adv. Mater. 22 (2010) 3906–3924.

[18] M. Zhou, Y. Zhai, and S. Dong, Anal. Chem. 81 (2009) 5603–5613.

[19] Y. Shao, J. Wang, H. Wu, J. Liu, I.A. Aksay, Y. Lin, Electroanalysis 22 (2010) 1027–1036.

[20] M. Pumera, A. Ambrosi, A. Bonanni, E.L.K. Chng, H.L. Poh, Trends in Anal. Chem. 29 (2010) 954–965.

[21] S. Pei, H. Cheng, CARBON 50 (2012) 3210–3228.

[22] S.Y. Toh, K.S. Loh, S.K. Kamarudin, W.R.W. Daud, J. Chem Eng., 251 (2014) 422–434.

[23] Y. Wang, Z. Shi and J. Yin, ACS Appl. Mater. Interfaces, 3 (2011) 1127–1133.

[24] D. Mhamane, W. Ramadan, M. Fawzy, A. Rana, M. Dubey, C. Rode, B. Lefez, B. Hannoyerd, S. Ogale, Green Chem. 13 (2011) 1990–1996.

[25] P. Gnanaprakasam, T. Selvaraju, RSC Adv. 4 (2014) 24518-24525.

[26] L. Wang, E. Wang, Electrochem. Commun., 6 (2004) 225–229.

[27] K.C. Lin, T.H. Wu, S.M. Chen, RSC Adv. 5 (2015) 41224–41229.

[28] A.A. Ensafi, M. M. Abarghoui, B. Rezaei, Sens. Actuators, B, 196 (2014) 398–405.

[29] E.C. Hurdis, H. Romeyn, Anal. Chem. 26 (1954) 320–325.

[30] N. Higashi, H. Yokota, S. Hiraki, Y. Ozaki, Ana. Chem. 77 (2005) 2272–2277.

[31] M.C.Y. Chang, A. Pralle, E.Y. Isacoff, C.J. Chang, J. Am. Chem. Soc. 126 (2004) 15392–15393.

[32] J. Lu, C. Lau, M. Morizono, K. Ohta, M. Kai, Anal. Chem. 73 (2001) 5979–5983.

[33] S. Palanisamy, S.M. Chen, R. Sarawathi, Sens. Actuators, B, 166–167 (2012) 372–377.

[34] J. Liu, C. Guo, C.M. Li, Y. Li, Q. Chi, X. Huang, L. Liao, T. Yu, Electrochem. Commun. 11 (2009) 202–205.

[35] Q. Rui, K. Komori, Y. Tian, H. Liu, Y. Luo, Y. Sakai, Anal. Chim. Acta 670 (2010) 57–62.

[36] S. Chen, R. Yuan, Y. Chai, L. Zhang, N. Wang, X. Li, Biosens. Bioelectron. 22 (2007) 1268–1274.

[37] C. Guo, F. Hua, C.M. Li, P.K. Shen, Biosens. Bioelectron. 24 (2008) 819–824.

[38] W. Chen , S. Cai , Q.Q. Ren , W. Wen, Y.D. Zhao, Analyst, 137 (2012) 49-58.

[39] S. Chen, R. Yuan, Y. Chai, F. Hu, Microchim. Acta 180 (2013) 15–32.

[40] R. Emmanuel, C. Karuppiah, S.M. Chen, S. Palanisamy, S. Padmavathy, P. Prakash, J. Hazard. Mater. 279 (2014) 117–124.

[41] H. Jabeen, V. Chandra, S. Jung, J.W. Lee, K.S. Kim, S.B. Kim, Nanoscale 3 (2011) 3583–3585.

[42] S. Yang, W. Yue, D. Huang, C. Chen, H. Lin, X. Yang, RSC Adv. 2 (2012) 8827–8832.

[43] N. Jia, B. Huang, L. Chen, L. Tan, S. Yao, Sens. Actuators, B, 195 (2014) 165–170.

[44] L. Luo, F. Li, L. Zhu, Z. Zhang, Y. Ding, D. Deng, Electrochim. Acta 77 (2012) 179–183.

[45] B.B. Jiang, X. W. Wei, F.H. Wu, & K.L. Wu, L. Chen, G.Z. Yuan, C. Dong, Y. Ye, Microchim. Acta, 181 (2014) 1463–1470.

[46] G. Yin, L. Xing, X. Ma, J. Wan, Chem. Pap., 68 (2014) 435–441.

[47] Z. Liu, B. Zhao, Y. Shia, C. Guo, H. Yang, Z. Li, Talanta 81 (2010) 1650–1654.

[48] S. Chairam, W. Sroysee, C. Boonchit, C. Kaewprom, T.G.N. Wangnoi, M. Amatatongchai, P. Jarujamrus, S. Tamaung, E. Somsook, Int. J. Electrochem. Sci., 10 **(**2015**)** 4611–4625.

Table 1 Comparison of analytical performance of as-prepared non-enzymatic H_2O_2 sensor (rGO/FeNPs nanocomposite modified electrode) with previously reported non-enzymatic H_2O_2 sensors.

Modified electrode	**pH**	**E_{app} (V)**	**Res. time (s)**	**LOD (µM)**	**Linear range (µM)**	**Ref.**
Fe@Pt CSNPs/GCE	7.0	–0.4	1.0	0.75	2.5–41605.0	**8**
MnO_2/OMC/GCE	8.0	0.45	3.0	0.07	0.5–600.0	**44**
Cu_2O/N-graphene/GCE	7.4	–0.6	2.0	0.8	5.0–3570.0	**45**
PtNPs/NPGE	7.5	0.4	–	0.72	0.1–20.0	**46**
Fe_3O_4–Ag/GCE	7.0	–0.5	3.0	1.2	1.2–3500.0	**47**
AgNPs/PABA/ Fe_3O_4/CPE	7.5	–0.4	5.0	1.74	5.0–5500.0	**48**
rGO/FeNPs/GCE	7.0	–0.5	2.0	0.056	0.1–2150.0	This work

Abbreviations:

E_{app} – Working potential; Res. Time – response time; LOD – limit of detection; CSNPs – core shell nanoparticles; GCE – glassy carbon electrode; OMC – mesoporous carbon; NPs – nanoparticles; NPGE – nano porous gold electrode; PABA – poly(o-aminobenzoic acid; CPE – carbon paste electrode.

Table 2 Determination of H_2O_2 in human blood serum, urine and commercial contact lens solution samples using rGO/FeNPs nanocomposite modified electrodes by amperometry. (n=3)

Sample	Spiked (μM)	Found (μM)	Recovery (%)	RSD
Commercial contact lens solution	–	13.49	–	–
	2.0	1.97	98.5	3.8
Human blood serum	–	–	–	–
	3.0	2.92	97.3	4.3
Human urine	–	–	–	–
	3.0	3.03	101.0	3.2

Figure captions

Scheme 1 A schematic representation for the green synthesis of rGO/FeNPs nanocomposite using IPTLE.

Figure 1 TEM images of FeNPs (A) rGO (B) and rGO/FeNPs nanocomposite (C). D) EDX spectrum of rGO/FeNPs nanocomposite.

Figure 2 A) FTIR spectra of IPTLE extract. B) FTIR spectra of GO (blue profile), rGO (black profile) and rGO/FeNPs nanocomposite (red profile).

Figure 3 XRD pattern of GO (a), rGO (b), FeNPs (c) and rGO/FeNPs nanocomposite (d).

Figure 4 A) CV response of bare (a), FeNPs (b), rGO (c) and rGO/FeNPs nanocomposite (d) modified electrodes in N_2 saturated PBS containing 1 mM H_2O_2 at a scan rate of 50 mV/s. Inset shows the effect of drop coating amount of rGO/FeNPs nanocomposite towards the current response for sensing of 1 mM H_2O_2. B) In the same conditions, CV response obtained for rGO/FeNPs nanocomposite modified electrode in the absence (a) and presence (b) of 1 mM H_2O_2 in N_2 saturated PBS; Scan rate = 50 mV/s.

Figure 5 A) CV response obtained at rGO/FeNPs nanocomposite modified electrode in N_2 saturated 1 mM H_2O_2 containing PBS at different scan rates; Scan rates in the range from 20 to 180 mV/s. Inset is the linear plot for square root of scan rate vs. current response of H_2O_2. B) The effect of pH on the catalytic activity of rGO/FeNPs nanocomposite towards sensing of 1 mM H_2O_2. The experimental conditions are similar to Fig. 5A.

Figure 6 Amperometric i-t response of rGO/FeNPs nanocomposite modified RDE for the addition of different concentrations of H_2O_2 into the constant stirred N_2 saturated PBS. Working potential = -0.5 V. Inset (upper) shows an enlarged view of amperometric response of the modified electrode

for the addition of 0.1 (a), 0.5 (b), 1 (c), 5 (d), 15 (e) and 50 (f) μM of H_2O_2 into the constant stirred PBS. Inset (lower) shows linear plot for current response vs. [H_2O_2].

Figure 7 Amperometric i-t response of rGO/FeNPs nanocomposite modified RDE for the addition of 1 μM H_2O_2 (a), and 100 μM of DA (b), UA (c), catechol (d), AA (e) and glucose (f) into the constant stirred N_2 saturated PBS at a working potential of -0.5 V.

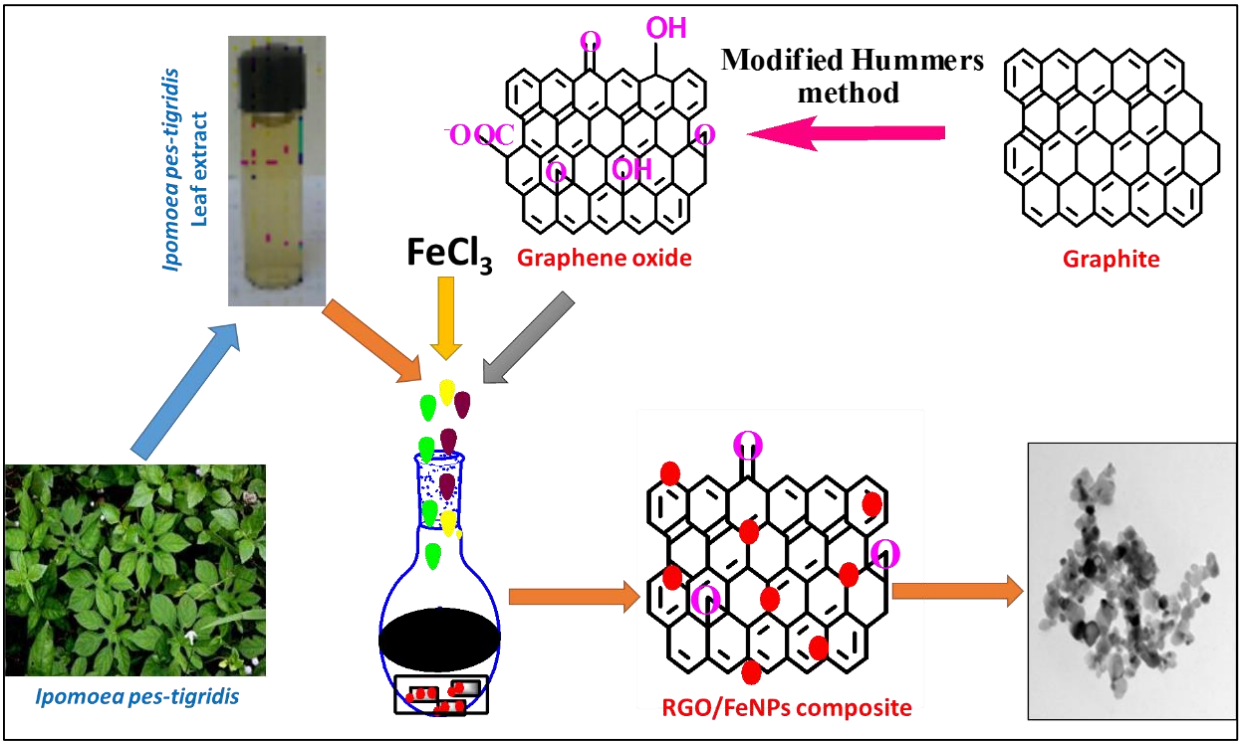
Ipomoea pes-tigridis
Leaf extract
Modified Hummers method
Graphite
Graphene oxide
FeCl3
Ipomoea pes-tigridis
RGO/FeNPs composite

Scheme–1

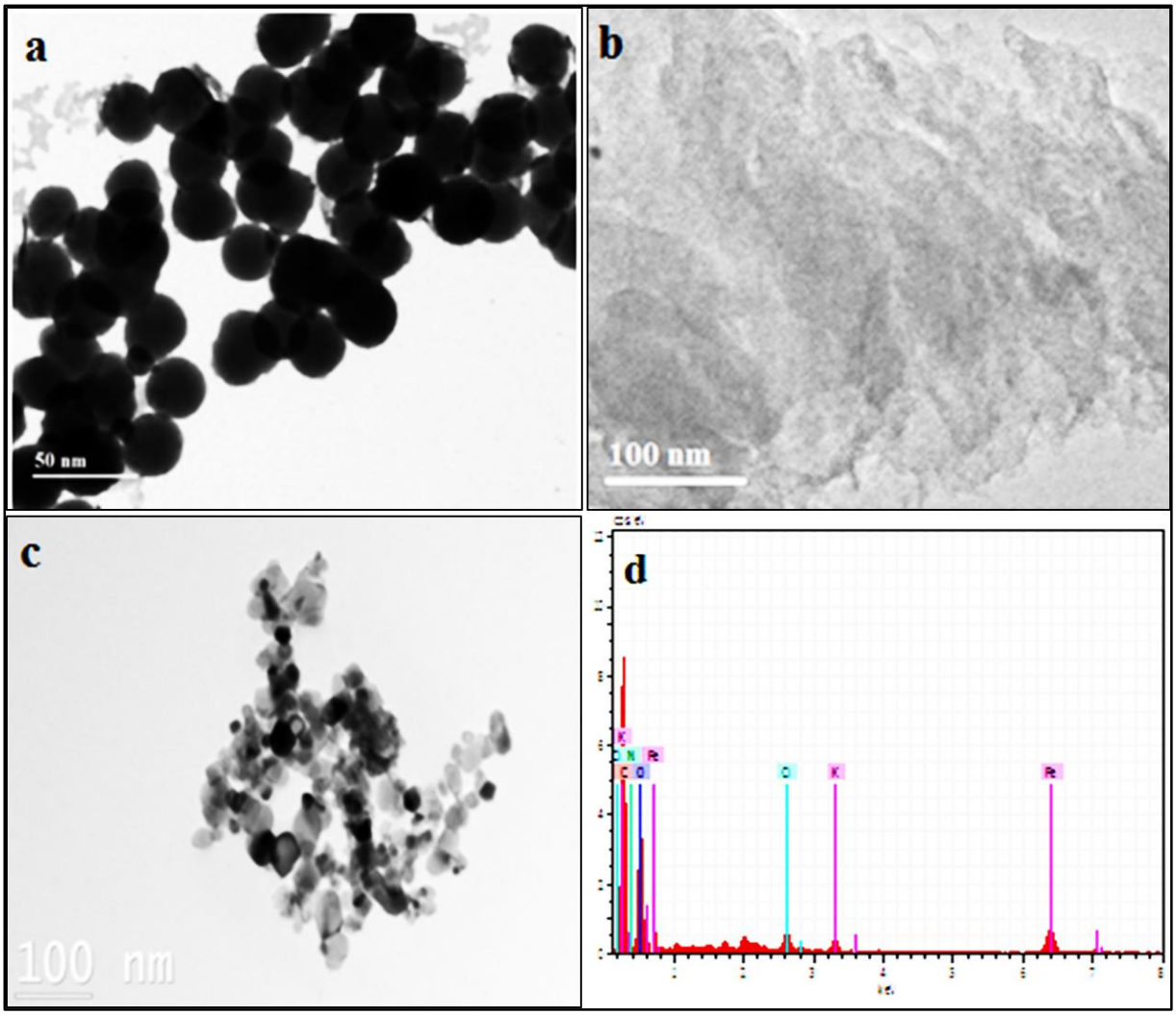

Figure–1

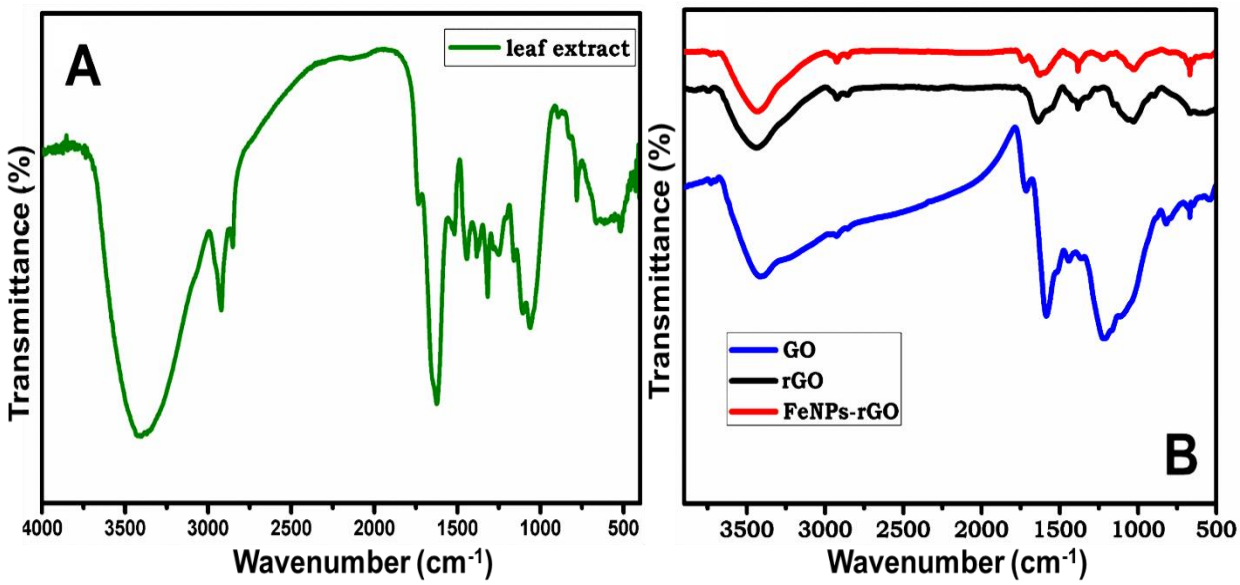
A
leaf extract
Transmittance (%)
4000
3500
3000
2500
2000
1500
1000
500
Wavenumber (cm-1)
B
GO
rGO
FeNPs-rGO
Transmittance (%)
3500
3000
2500
2000
1500
1000
500
Wavenumber (cm-1)

Figure-2

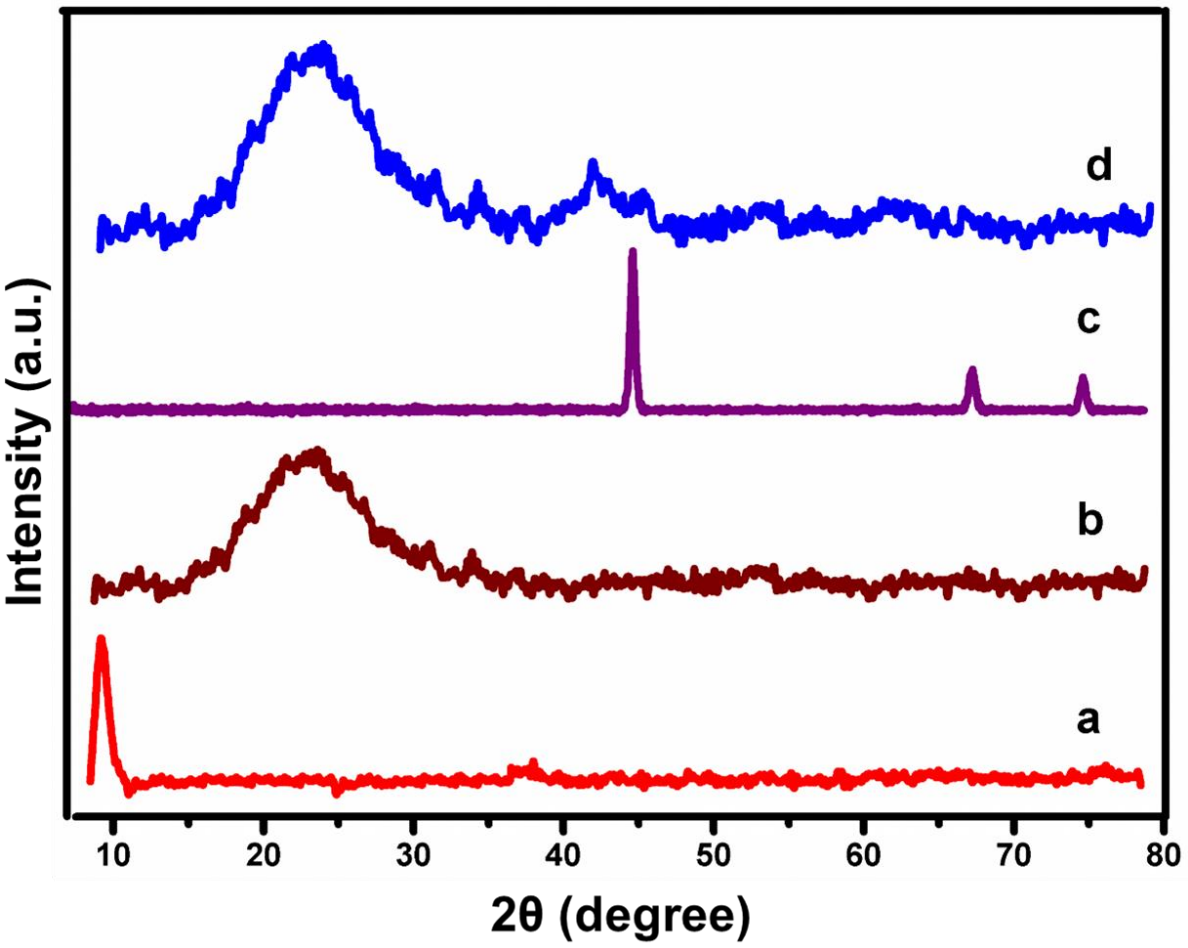

Figure-3

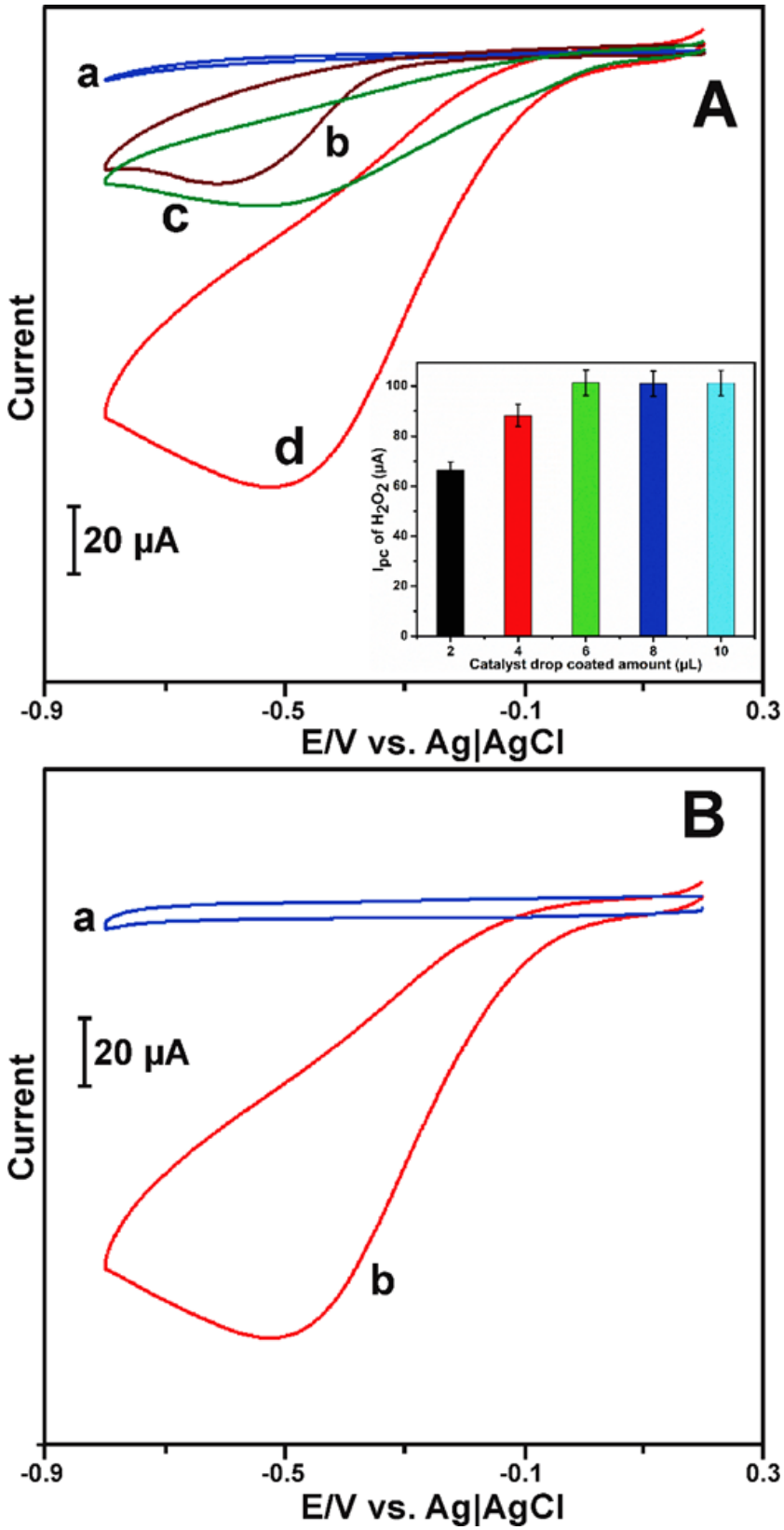
A
a
b
c
d
20 μA
Current
-0.9
-0.5
-0.1
0.3
E/V vs. Ag|AgCl
I_{pc} of H_2O_2 (μA)
Catalyst drop coated amount (μL)
B
a
b
20 μA
Current
-0.9
-0.5
-0.1
0.3
E/V vs. Ag|AgCl

Figure–4

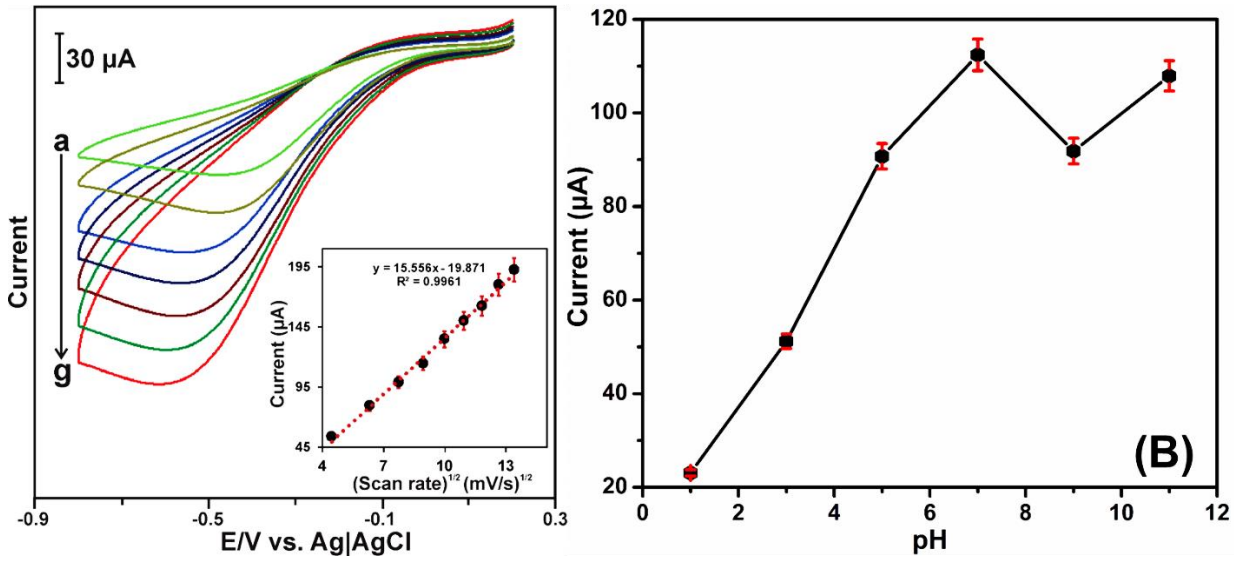
30 µA
a
g
Current
E/V vs. Ag|AgCl
-0.9
-0.5
-0.1
0.3
y = 15.556x - 19.871
R² = 0.9961
Current (µA)
(Scan rate)^1/2 (mV/s)^1/2
Current (µA)
pH
(B)

Figure–5

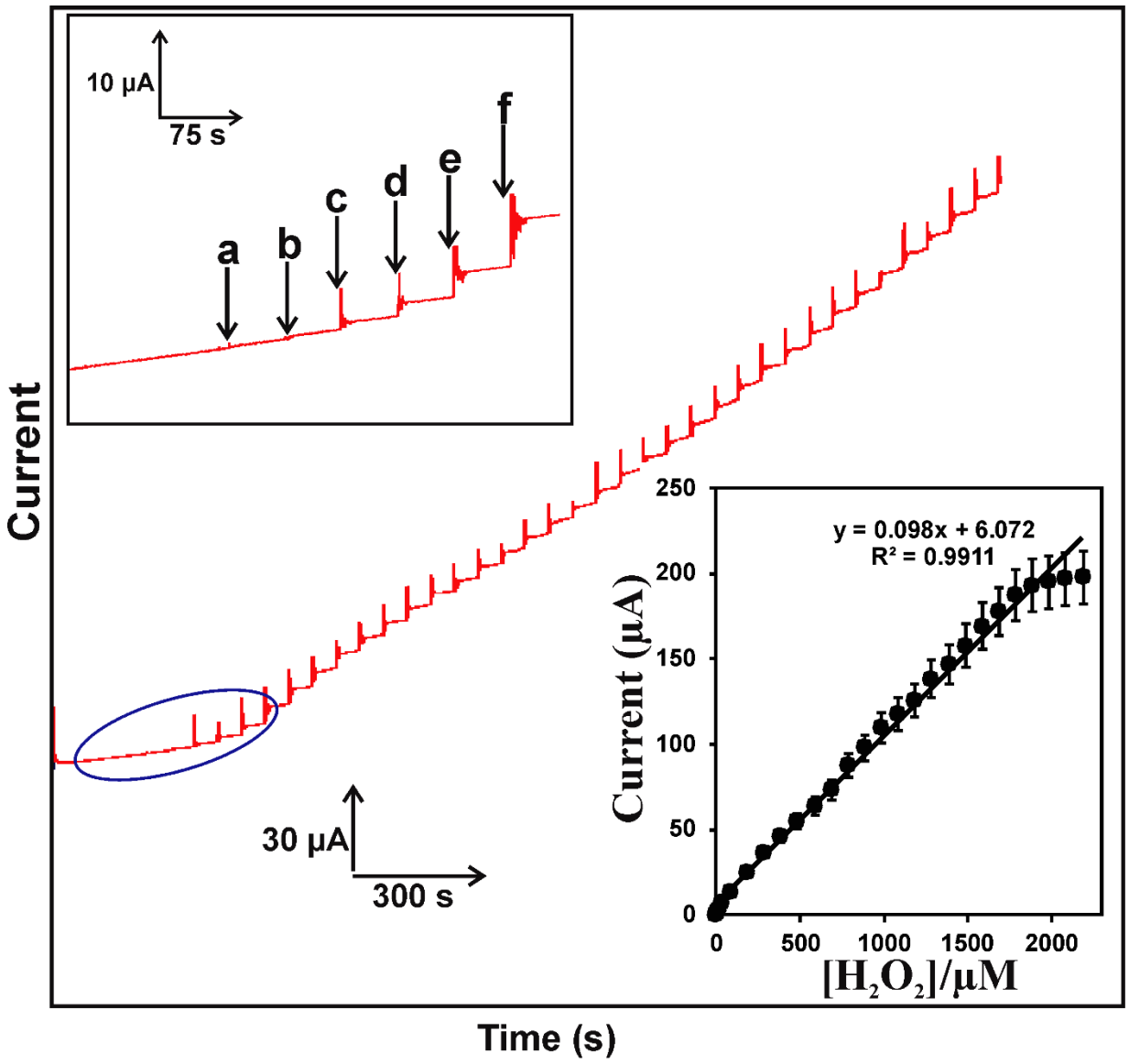
10 µA
75 s
a
b
c
d
e
f
Current
30 µA
300 s
Time (s)
y = 0.098x + 6.072
R² = 0.9911
Current (µA)
[H2O2]/µM
0
50
100
150
200
250
0
500
1000
1500
2000

Figure–6

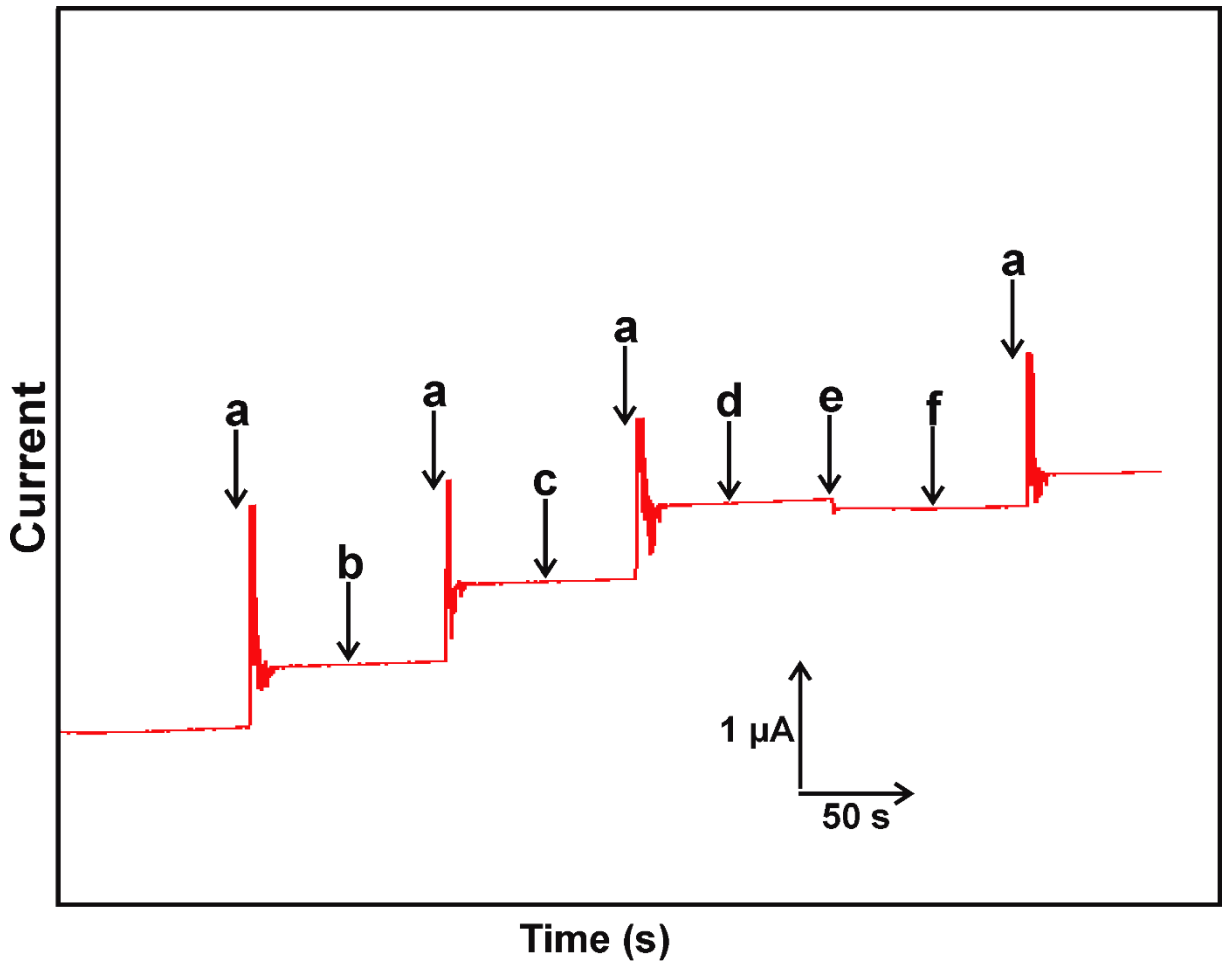

Figure–7